



DIGITAL ACCESS TO
SCHOLARSHIP AT HARVARD
DASH.HARVARD.EDU



HARVARD LIBRARY
Office for Scholarly Communication

Oxygenation of the mid-Proterozoic atmosphere: clues from chromium isotopes in carbonates

The Harvard community has made this article openly available. [Please share](#) how this access benefits you. Your story matters

Citation	Gilleaudeau, G.J., R. Frei, A.J. Kaufman, L.C. Kah, K. Azmy, J.K. Bartley, P. Chernyavskiy, and A.H. Knoll. 2016. "Oxygenation of the Mid-Proterozoic Atmosphere: Clues from Chromium Isotopes in Carbonates." <i>Geochemical Perspectives Letters</i> : 178–187. doi:10.7185/geochemlet.1618.
Published Version	doi:10.7185/geochemlet.1618
Citable link	http://nrs.harvard.edu/urn-3:HUL.InstRepos:33973839
Terms of Use	This article was downloaded from Harvard University's DASH repository, and is made available under the terms and conditions applicable to Open Access Policy Articles, as set forth at http://nrs.harvard.edu/urn-3:HUL.InstRepos:dash.current.terms-of-use#OAP

1 **Oxygenation of the mid-Proterozoic atmosphere: clues from chromium isotopes in**
2 **carbonate rocks**

3

4 Geoffrey J. Gilleaudeau^{1,*}, Robert Frei¹, Alan J. Kaufman², Linda C. Kah³, Karem
5 Azmy⁴, Julie K. Bartley⁵, Pavel Chernyavskiy⁶, Andrew H. Knoll⁷

6

7 ¹Department of Geosciences and Natural Resource Management, University of
8 Copenhagen, Øster Voldgade 10, 1350 Copenhagen, Denmark; ggillea1@gmail.com;
9 robertf@ign.ku.dk

10

11 ²Department of Geology, University of Maryland, College Park, MD 20742, USA;
12 kaufman@geol.umd.edu

13

14 ³Department of Earth and Planetary Sciences, University of Tennessee, Knoxville, TN
15 37996, USA; lckah@utk.edu

16

17 ⁴Department of Earth Sciences, Memorial University of Newfoundland, St. John's,
18 Newfoundland A1B 3X5, Canada; kazmy@mun.ca

19

20 ⁵Department of Geology, Gustavus Adolphus College, St. Peter, MN 56082, USA;
21 jbartley@gustavus.edu

22

23 ⁶Biostatistics/Radiation Epidemiology Branch, National Cancer Institute, National
24 Institutes of Health, Rockville, MD 20850, USA; pchern1@gmail.com

25

26 ⁷Department of Organismic and Evolutionary Biology, Harvard University, Cambridge,
27 MA 02138, USA; aknoll@oeb.harvard.edu

28

29 *Corresponding author: ggillea1@gmail.com

30 Current address: School of Earth and Space Exploration, Arizona State University,
31 Tempe, AZ 85281, USA

32

33 **Abstract**

34 Chromium (Cr) isotopes in marine sedimentary rocks can be used as a sensitive proxy for
35 ancient atmospheric oxygen because Cr-isotope fractionation during terrestrial
36 weathering only occurs when pO_2 exceeds a threshold value. This is a useful system
37 when applied to rocks of mid-Proterozoic age, where fundamental questions persist about
38 atmospheric pO_2 and its relationship to biological innovation. Whereas previous studies
39 have focused on temporally limited iron-rich sedimentary rocks, we present a pilot study
40 of Cr-isotopes in mid-Proterozoic marine carbonate rocks. Application of the Cr-isotope
41 proxy to carbonate rocks has the potential to greatly enhance the temporal resolution of
42 Proterozoic palaeo-redox data. Here we report positive $\delta^{53}Cr$ values in four carbonate
43 successions, extending the mid-Proterozoic record of Cr-isotope fractionation—and thus
44 pO_2 above threshold values—back to ~1.1 Ga. These data suggest that pO_2 sufficient for
45 the origin of animals was transiently in place well before their Neoproterozoic

46 appearance, although uncertainty in the pO_2 threshold required for Cr-isotope
47 fractionation precludes definitive biological interpretation. This study provides a proof of
48 concept that the Cr-isotopic composition of carbonate rocks can provide important new
49 constraints on the oxygen content of the ancient atmosphere.

50

51 **Introduction**

52 The chromium (Cr) isotope system functions as an atmospheric redox proxy because
53 oxidative weathering of crustal Cr(III)-bearing minerals results in the release of ^{53}Cr -
54 enriched mobile Cr(VI) to solution (Izbicki *et al.*, 2008). Cr(VI) (dominantly as
55 chromate; CrO_4^-) is then carried to the oceans via rivers, thus imparting a positively
56 fractionated $\delta^{53}\text{Cr}$ signal on modern seawater (+0.13 to +1.55‰ compared to crustal
57 values of $-0.123 \pm 0.102\text{‰}$) (Schoenberg *et al.*, 2008; Bonnand *et al.*, 2013; Scheiderich
58 *et al.*, 2015; Wang *et al.*, 2016; Paulukat *et al.*, *in prep.*). Terrestrial Cr(III)-oxidation
59 occurs by reaction with manganese (Mn) oxides (Oze *et al.*, 2007), and it is thought that
60 Mn-oxide formation requires a threshold level of O_2 in the atmosphere. Frei *et al.* (2016)
61 suggested that Cr-oxidation by Mn-oxides is thermodynamically possible at pO_2 as low
62 as 10^{-5} of the present atmospheric level (PAL). Kinetic considerations dictate, however,
63 that 0.1 to 1 % PAL is necessary to oxidize Cr(III) within typical soil residence times
64 (Planavsky *et al.*, 2014) and between 0.03 and 0.3 % PAL is necessary to export Cr
65 without re-reduction by Fe(II) (Crowe *et al.*, 2013). Thus, the Cr-isotope system serves as
66 a sensitive binary indicator of atmospheric pO_2 above or below these threshold values.
67 Upon entering the marine environment, Cr(VI) can be reduced back to particle-reactive
68 Cr(III)—a process that preferentially utilizes ^{52}Cr , leaving residual Cr(VI) ^{53}Cr -enriched.

69 As a result, differing degrees of *in situ* Cr-reduction control Cr-isotope heterogeneity in
70 the modern oceans (Scheiderich *et al.*, 2015; Paulakut *et al.*, *in prep.*).

71

72 Because terrestrial Cr-oxidation is sensitive to atmospheric oxygen, the Cr-isotope
73 composition of seawater through time—as recorded in marine sedimentary rocks—is a
74 potentially powerful tool for reconstructing ancient atmospheric pO_2 . This is particularly
75 useful for testing hypotheses about atmospheric oxygenation during the Proterozoic Eon,
76 where fundamental questions persist about the O_2 content of Earth's atmosphere and its
77 relationship to temporal patterns of biological innovation.

78

79 The oxygenation of Earth surface environments was a protracted process that occurred
80 over >2 billion years (Ga). Two first-order oxygen pulses have been identified from the
81 Proterozoic geologic record. During the Great Oxidation Event (GOE) at ~2.4 Ga, pO_2
82 was sustained above 10^{-5} PAL for the first time in Earth history (Pavlov and Kasting,
83 2002), although transient 'whiffs' of O_2 have been recognized from the Archaean
84 geochemical record (Anbar *et al.*, 2007). During a subsequent Neoproterozoic
85 oxygenation event (NOE) at ~635-550 Ma, pO_2 began to rise to near-modern levels—a
86 transition that continued into the Palaeozoic Era (Och and Shields-Zhou, 2012).

87

88 Empirical constraints remain limited, however, on pO_2 during the prolonged period in
89 between. Constraining pO_2 during the mid-Proterozoic Eon has major implications for
90 understanding potential biogeochemical controls on the timing of animal diversification.
91 Some argue that exceedingly low mid-Proterozoic pO_2 was a direct impediment to

92 metazoan evolution prior to the Neoproterozoic Era (Lyons *et al.*, 2014; Planavsky *et al.*,
93 2014; Tang *et al.*, 2016), whereas others argue that oxygen levels required by early
94 animals were in place long before their Neoproterozoic appearance (Butterfield, 2009;
95 Mills *et al.*, 2014; Zhang *et al.*, 2016). Mid-Proterozoic Cr-isotope data have the potential
96 to inform this debate because estimates of the pO_2 threshold needed for Cr-isotope
97 fractionation are roughly similar to experimental and theoretical estimates of the O_2
98 requirements of early animals (0.3 to 4 % PAL) (Levin, 2003; Palma *et al.*, 2005;
99 Sperling *et al.*, 2013a; Mills *et al.*, 2014).

100

101 Thus far, studies have largely focused on iron-rich sedimentary rocks as an archive for
102 ancient seawater $\delta^{53}Cr$ values (Planavsky *et al.*, 2014; Frei *et al.*, 2009; 2016). In the
103 presence of Fe(II), seawater Cr(VI) is reduced to Cr(III) and can be co-precipitated with
104 Fe-oxyhydroxides (Døssing *et al.*, 2011). Cr reduction favors the light ^{52}Cr isotope, so
105 that iron-rich rocks record seawater $\delta^{53}Cr$ values only if Cr reduction is quantitative.
106 Ironstone and iron formation data have thus far provided important constraints on
107 Archaean ‘whiffs’ of oxygen and the subsequent GOE, as well as new clues about the
108 NOE (Frei *et al.*, 2009; Planavsky *et al.*, 2014). Sparse ironstone data from the mid-
109 Proterozoic suggest a lack of Cr-isotope fractionation (Planavsky *et al.*, 2014). Iron-rich
110 rocks are rare in mid-Proterozoic successions, however, limiting our ability to generate
111 data for the crucial period preceding the NOE.

112

113 The impetus of this study, then, is to test the reliability of Cr-isotopes in an alternative
114 lithology (marine carbonate rocks) that is ubiquitous in the mid-Proterozoic geologic

115 record. A potential advantage of using carbonate rocks as a Cr-isotope archive is that
116 chromate can be incorporated into the lattice of carbonate minerals with no change in
117 oxidation state. Studies of modern invertebrate shells (coral, bivalves, gastropods) reveal
118 that Cr-isotope fractionation does occur during biomineralization, making skeletal
119 carbonates an unreliable archive of seawater $\delta^{53}\text{Cr}$ values (Paulukat *et al.*, 2015; Pereira
120 *et al.*, 2016). Mohanta *et al.* (2016) showed that modern bulk biogenic carbonate is as
121 much as 0.45 ‰ lighter than seawater. Co-precipitation experiments involving chromate
122 incorporation into calcite have shown, however, that abiogenic carbonate has the
123 potential to record $\delta^{53}\text{Cr}$ values of the ambient solution (Rodler *et al.*, 2015). In
124 experiments with the lowest initial Cr concentration (8.6 ppm), precipitates were <0.1 ‰
125 heavier than the solution, suggesting that minimal fractionation occurs during chromate
126 incorporation into calcite at low Cr concentrations typical of seawater (0.08 to 0.5 ppm;
127 Scheiderich *et al.*, 2015; Paulukat *et al.*, *in prep.*).

128

129 In this study, we measured the Cr-isotopic composition of marine limestone and
130 dolostone from four geographically distinct mid-Proterozoic successions, along with a
131 suite of major and trace elements to constrain diagenetic pathways and the influence of
132 detrital contamination. We focused on the interval between ~1.1 and 0.9 Ga—where sea
133 level highstand resulted in marine carbonate deposition across multiple cratons—and a
134 variety of depositional environments to assess the consistency and reliability of the
135 proxy. Our data are discussed in the context of best practices regarding diagenesis and
136 detrital contamination, and ultimately, used to provide important new constraints on
137 atmospheric $p\text{O}_2$ during the mid-Proterozoic Eon.

138

139 **Geologic Background**

140 Samples were analyzed from the Turukhansk Uplift, Siberia (~900-1035 Ma), the
141 Angmaat Formation, Canada (~1092 Ma), the El Mreiti Group, Mauritania (~1107 Ma),
142 and the Vazante Group, Brazil (~1112 Ma). Detailed description of the geologic setting,
143 depositional environments, geochronology, and post-depositional history of each
144 succession can be found in the Supplementary Information.

145

146 **Analytical Methods**

147 Chromium separation and isotopic analysis techniques were modified from Pereira *et al.*
148 (2016). All Cr-isotope and Cr concentration measurements were performed at the
149 University of Copenhagen on a thermal ionization mass spectrometer (TIMS). Ca, Mg,
150 Fe, Sr, Mn, and Al concentrations were measured by ICP-OES on splits of the same
151 solutions used for Cr-isotopic analysis. Ti and Zr concentrations were measured by ICP-
152 MS at the Geological Survey of Denmark and Greenland. Additional detail can be found
153 in the Supplementary Information.

154

155 **Diagenetic Considerations**

156 Carbonate minerals are reactive in the diagenetic environment so that care must be taken
157 in selecting the best-preserved samples for isotopic analysis. Criteria for sample inclusion
158 were based upon conventional petrography, carbon and oxygen isotope compositions, and
159 trace element concentrations. Micritic to microsparitic textures characterize most
160 samples, with the exception of discrete intervals of alteration that were excluded (Figs.

161 SI-1, SI-2). Similarly, $\delta^{13}\text{C}$, $\delta^{18}\text{O}$, and trace element signatures are in line with typical
162 least-altered mid-Proterozoic limestone and dolostone (Kah *et al.*, 1999) with some
163 exceptions that were considered altered, and thus excluded (Fig. SI-3). A total of 17
164 samples were excluded based on diagenetic criteria, including 13 from the Vazante
165 Group. Interestingly, samples that are considered altered—with lower than average $\delta^{18}\text{O}$
166 values—tend to have unfractionated $\delta^{53}\text{Cr}$ values that approach average crust (-0.12‰)
167 (Fig. SI-4). This may indicate that discrete intervals of alteration (particularly in the
168 Vazante Group) were characterized by a resetting of the $\delta^{53}\text{Cr}$ signal to crustal values.
169 Future study should investigate this possibility, but for the purposes of this study, these
170 samples were excluded based on standard diagenetic criteria. Additional textural and
171 geochemical information can be found in the Supplementary Information.

172

173 The only previously published study on Cr-isotopes in carbonate rocks (Frei *et al.*, 2011)
174 demonstrated stratigraphic $\delta^{53}\text{Cr}$ trends that mirror primary $\delta^{13}\text{C}$ trends across a mixed
175 limestone-dolostone interval. Because the C-isotope signal is thought to reflect seawater,
176 co-variation with $\delta^{53}\text{Cr}$ speaks to the fidelity potential of Cr-isotopes in both limestone
177 and dolostone and suggests that, in the absence of further study on Cr-isotope behavior
178 during diagenesis, standard petrographic and geochemical criteria can be used as a
179 starting point for Cr-isotope diagenetic screening.

180

181 **Detrital Chromium Contamination**

182 Our results indicate a broad range of $\delta^{53}\text{Cr}$ values in each succession, ranging from
183 crustal values (near -0.12‰) to strongly positive values (up to $+1.77\text{‰}$). To understand

184 this isotopic heterogeneity, we first evaluated the degree to which measured $\delta^{53}\text{Cr}$ values
185 reflect authigenic Cr in carbonate vs. allogenic Cr from detrital sources. As part of each
186 dissolution for $\delta^{53}\text{Cr}$ analysis, we measured a split for aluminum (Al) content to assess
187 the degree to which clay—which can be a host phase for detrital Cr—was leached during
188 dissolution. In a plot of Al concentration in the leachate vs. measured $\delta^{53}\text{Cr}$ values (Fig.
189 1A), positively fractionated $\delta^{53}\text{Cr}$ is only recorded in samples where less than ~400 ppm
190 Al is leached. A similar trend is observed for other detrital indicators. Positively
191 fractionated $\delta^{53}\text{Cr}$ is only observed when leachate titanium (Ti) and zirconium (Zr)
192 concentrations are generally less than 10 and 1 ppm, respectively (Fig. SI-5), although the
193 relationship is not well-defined for Zr. Assuming that Al is the most effective indicator of
194 clay contamination, we compared sample Cr/Al ratios to an average shale composite (Cr
195 = 90 ppm; Al = 8.89 wt. %; Wedepohl, 1991)—which serves as a first-order proxy for
196 clay-rich detrital sediment—to derive a rough estimate of the fraction of Cr sourced from
197 detrital material for each sample. Similarly, positively fractionated $\delta^{53}\text{Cr}$ is only recorded
198 in samples where less than ~35 % of measured Cr is detritally sourced (Fig. 1B).

199

200 These trends represent a mixing curve where Cr in the carbonate lattice is dissolved and
201 analyzed in addition to Cr leached from clay. When detrital Cr exceeds ~35 % of total
202 measured Cr, $\delta^{53}\text{Cr}$ values approach average crust (-0.12 ‰) and the isotopic
203 composition of the authigenic seawater component is unresolvable. When samples have
204 less than ~35 % detrital Cr, we can perform a basic correction of measured $\delta^{53}\text{Cr}$ values,
205 assuming the detrital component has a crustal $\delta^{53}\text{Cr}$ value. This yields a first-order
206 estimate of the isotopic composition of the authigenic Cr component ($\delta^{53}\text{Cr}_{\text{auth}}$), which is

207 derived from seawater (see Supplementary Information). We also performed corrections
208 using post-Archaean Australian shale (PAAS) values (Taylor and McLennan, 1985)
209 instead of the average shale composite of Wedepohl (1991), but found <2 % differences
210 in estimates of detrital Cr contribution and < 0.02 ‰ differences in corrected $\delta^{53}\text{Cr}_{\text{auth}}$
211 values.

212

213 After exclusion of samples based on diagenetic and detrital contamination criteria, our
214 dataset consisted of 62 samples that cover all four successions. These methods for
215 assessing detrital Cr contamination represent a new set of best practices that should be
216 applied in future studies that examine the Cr-isotopic composition of carbonate rocks.

217

218 **Constraining Atmospheric Oxygen**

219 The main observation of our dataset is that all four successions record positively
220 fractionated $\delta^{53}\text{Cr}_{\text{auth}}$ values. The maximum isotopic difference observed by Rodler *et al.*
221 (2015) between synthetic calcite and ambient solution was 0.33 ‰ so that, even if some
222 fractionation did occur during carbonate formation, the preponderance of strongly
223 positive $\delta^{53}\text{Cr}$ values in our dataset (n = 24 samples >0.3 ‰) indicate that mid-
224 Proterozoic seawater was positively fractionated. Additionally, if carbonate preferentially
225 incorporated ^{52}Cr as observed by Mohanta *et al.* (2016), then our dataset provides even
226 stronger evidence for positively fractionated Cr in mid-Proterozoic seawater.

227

228 The record of positively fractionated Cr in seawater has recently been extended back to
229 ~3.8 Ga, which Frei *et al.* (2016) interpret as terrestrial Cr-oxidation under an otherwise

230 anoxic Archaean atmosphere. Banded iron formations from the Archaean-Proterozoic
231 transition record pulses of terrestrial Cr-oxidation prior to the GOE and a lack of Cr-
232 isotope fractionation immediately following the GOE, which is interpreted as a post-GOE
233 decline in atmospheric pO_2 (Frei *et al.*, 2009). Subsequent evidence for Cr-isotope
234 fractionation is not found until ~750 Ma (Planavsky *et al.*, 2014), leading to the
235 suggestion that persistently low pO_2 inhibited Cr-isotope fractionation during the entire
236 mid-Proterozoic Eon. Here we extend the mid-Proterozoic record of positively
237 fractionated Cr back to ~1.1 Ga—a revision of ~350 Ma from previous estimates (Fig. 2).

238

239 At present, there is no clear consensus on the pO_2 level required for Cr-isotope
240 fractionation during terrestrial weathering (*e.g.*, Crowe *et al.*, 2013; Planavsky *et al.*,
241 2014; Frei *et al.*, 2016). If we take soil residence time calculations (~0.1 to 1 % PAL;
242 Planavsky *et al.*, 2014) as our best estimate, we conclude that pO_2 at least transiently
243 exceeded ~0.1 to 1 % PAL during the mid-Proterozoic Eon. These data are consistent
244 with a broad range of proxies that suggest mild biospheric oxygenation in the
245 Mesoproterozoic Era (Kah *et al.*, 1999; 2001; 2004; Frank *et al.*, 2003; Johnston *et al.*,
246 2005; Parnell *et al.*, 2010; Spinks *et al.*, 2014; Zhang *et al.*, 2016). Data are potentially
247 inconsistent, however, with recent estimates of pO_2 persistently between or below 0.1 to
248 1 % PAL throughout the entire mid-Proterozoic Eon (Lyons *et al.*, 2014; Liu *et al.*, 2016;
249 Tang *et al.*, 2016), including Cr-isotope data from sparse mid-Proterozoic iron oolites
250 (Planavsky *et al.*, 2014).

251

252 Conflict between our data and other proxies could be related to uncertainty regarding the
253 pO_2 threshold required for Cr-isotope fractionation. If we take 0.03 % PAL as the
254 required threshold (Crowe *et al.*, 2013), for example, our data become compatible with
255 the pO_2 estimate of Liu *et al.* (2016) based on carbonate Zn/Fe systematics. Regardless of
256 the threshold value, however, our data remain inconsistent with Cr-isotope data from
257 mid-Proterozoic iron oolites (Planavsky *et al.*, 2014). This discrepancy cannot be
258 explained by Cr-isotope fractionation during carbonate formation, particularly if
259 carbonates preferentially incorporate ^{52}Cr (Mohanta *et al.*, 2016), which would only
260 amplify evidence for positively fractionated Cr in mid-Proterozoic seawater. Carbonate
261 diagenesis can also be excluded because least-altered samples in our dataset have positive
262 $\delta^{53}Cr$ values and, in samples where there is evidence for diagenesis, unfractionated $\delta^{53}Cr$
263 values are recorded. This indicates that—at least in our dataset—diagenesis is more likely
264 to give a false negative than a false positive result. Another possibility is that ironstone
265 data do not record seawater $\delta^{53}Cr$ because of partial Cr-reduction during precipitation of
266 shallow water iron oolites, which may have occurred under fluctuating redox conditions.
267 As articulated by Planavsky *et al.* (2014), however, this would be expected to generate a
268 range of $\delta^{53}Cr$ values—not the persistently unfractionated values that were measured.

269

270 Another alternative is that mid-Proterozoic pO_2 was variable around the threshold
271 required for Cr-isotope fractionation. There is evidence for this in our dataset—the
272 persistence of unfractionated $\delta^{53}Cr$ values that are not related to detrital contamination
273 (Fig. 1) could be related to transient periods of pO_2 below threshold values. Indeed the
274 only measured iron oolites that temporally overlap with samples from this study are

275 limited samples from the ~0.9 Ga Aok Formation (Canada), implying that the coarse
276 temporal resolution of current data may be insufficient to track short-term variability in
277 pO_2 . Data from earlier Proterozoic carbonate successions are needed to further test the
278 hypothesis of Planavsky *et al.* (2014). Taken together with the full range of published
279 proxy data (Frank *et al.*, 2003; Kah *et al.*, 2004; Johnston *et al.*, 2005; Parnell *et al.*,
280 2010; Planavsky *et al.*, 2014; Liu *et al.*, 2016; Tang *et al.*, 2016; Zhang *et al.*, 2016), we
281 conclude that mid-Proterozoic pO_2 was likely more dynamic than previously envisaged.

282

283 **Biological Implications**

284 Implications of our data on biospheric evolution are similarly tied to uncertainty
285 regarding the pO_2 threshold needed for Cr-isotope fractionation. Tank experiments have
286 shown that sponges can survive when pO_2 is as low as 0.5 to 4 % PAL, leading Mills *et*
287 *al.* (2014) to conclude that this level was likely sufficient for the origin of animals. Based
288 on theoretical early annelid body plans, a small worm with a circulatory system could
289 likely survive at pO_2 as low as 0.14 % PAL (Sperling *et al.*, 2013a). Studies from modern
290 oxygen minimum zones confirm these estimates and suggest that the bilaterian body plan
291 would only be inhibited if pO_2 were below 0.4 % PAL (Levin, 2003; Palma *et al.*, 2005;
292 Sperling *et al.*, 2013a). If we take 0.1 to 1 % PAL as the threshold required for Cr-isotope
293 fractionation (Planavsky *et al.*, 2014), then our data suggest that pO_2 levels sufficient for
294 the origin of animals were at least transiently in place by ~1.1 Ga—some 300 Ma before
295 the origin of sponges based on molecular clock estimates (Erwin *et al.*, 2011) and >450
296 Ma before the first appearance of animals in the fossil record (Narbonne, 2005). By
297 contrast, if we take the lower threshold value of 0.03 % PAL proposed by Crowe *et al.*

298 (2013), then our data have less direct implications for biology. Ecological considerations
299 are also important and modern oxygen minimum zones suggest that there is a clear
300 linkage between oxygen availability, animal size, and the relative proportion of
301 carnivorous taxa (Sperling *et al.*, 2013b). Based on these considerations it seems that,
302 although the oxygen requirements of small, simple animals were likely met by ~1.1 Ga,
303 low atmospheric pO_2 may still have inhibited the development of larger, more energetic
304 animals that have greater preservation potential in the fossil record.

305

306 **Conclusions and Outlook**

307 This pilot study demonstrates the viability of the Cr-isotope palaeo-redox proxy as it is
308 applied to ancient carbonate rocks. Once best screening practices for diagenesis and
309 detrital contamination are applied, Cr-isotope data can be interpreted in the context of
310 ancient atmospheric pO_2 . Results from four carbonate successions extend the mid-
311 Proterozoic record of positively fractionated Cr back to ~1.1 Ga—a revision of ~350 Ma
312 from previous estimates. If we take 0.1 to 1 % PAL as the pO_2 threshold needed for Cr-
313 isotope fractionation, then our data suggest that the oxygen requirements of small, simple
314 animals were at least transiently met well prior to their Neoproterozoic appearance,
315 although uncertainty regarding this pO_2 threshold precludes definitive biological
316 interpretation. Ultimately, the development of novel carbonate-based redox proxies has
317 the potential to greatly enhance the temporal resolution of palaeo-redox data for the
318 Proterozoic Eon.

319

320 **Acknowledgements**

321 This work was supported by grants from the Danish Natural Science Research Council
322 (FNU) to R.F. and the Carlsberg Foundation to G.J.G. and R.F. A.H.K. thanks the NASA
323 Astrobiology Institute and G.J.G. thanks the NASA Postdoctoral Program. We are
324 indebted to Toni Larsen for help in ion chromatographic separation of Cr, Toby Leeper
325 for mass spectrometry support, Jørgen Kystol for running the ICP-MS, and Andrea
326 Vögelin for major contributions to Cr-isotope analytical and data interpretation
327 techniques. We also thank Clemens V. Ullmann for ICP-OES expertise and insightful
328 comments on an earlier draft of this manuscript.

329

330 **References**

331 Anbar, A.D. *et al.* (2007) A whiff of oxygen before the Great Oxidation Event? *Science*
332 **317**, 1903-1906.

333 Bonnard, P, James, R.H., Parkinson, I.J., Connelly, D.P., Fairchild, I.J. (2013) The
334 chromium isotopic composition of seawater and marine carbonates. *Earth Planet. Sci.*
335 *Lett.* **382**, 10-20.

336 Butterfield, N.J. (2009) Oxygen, animals and oceanic ventilation: an alternative view.
337 *Geobiology* **7**, 1-7.

338 Crowe, S.A. *et al.* (2013) Atmospheric oxygenation three billion years ago. *Nature* **501**,
339 535-538.

340 Døssing, L.N., Dideriksen, K., Stipp, S.L.S., Frei, R. (2011) Reduction of hexavalent
341 chromium by ferrous iron: a process of chromium isotope fractionation and its relevance
342 to natural environments. *Chem. Geol.* **285**, 157-166.

343 Erwin, D.H. *et al.* (2011) The Cambrian conundrum: early divergence and later

344 ecological success in the early history of animals. *Science* **334**, 1091-1097.

345 Frank, T.D., Kah, L.C., Lyons, T.W. (2003) Changes in organic matter production and
346 accumulation as a mechanism for isotopic evolution in the Mesoproterozoic ocean. *Geol.*
347 *Magazine* **140**, 397-420.

348 Frei, R. *et al.* (2016) Oxidative elemental cycling under the low O₂ Eoarchean
349 atmosphere. *Scientific Reports* **6**, 21058.

350 Frei, R., Gaucher, C., Poulton, S.W., Canfield, D.E. (2009) Fluctuations in Precambrian
351 atmospheric oxygenation recorded by chromium isotopes. *Nature* **461**, 250-253.

352 Frei, R., Gaucher, C., Døssing, L.N., Sial, A.N. (2011) Chromium isotopes in
353 carbonates—a tracer for climate change and for reconstructing the redox state of ancient
354 seawater. *Earth Planet. Sci. Lett.* **312**, 114-125.

355 Gilleaudeau, G.J., Kah, L.C. (2013) Oceanic molybdenum drawdown by epeiric sea
356 expansion in the Mesoproterozoic. *Chem. Geol.* **356**, 21-37.

357 Gilleaudeau, G.J., Kah, L.C. (2015) Heterogeneous redox conditions and a shallow
358 chemocline in the Mesoproterozoic ocean: evidence from carbon-sulfur-iron
359 relationships. *Precambrian Res.* **257**, 94-108.

360 Izbicki, J.A., Ball, J.W., Bullen, T.D., Sutley, S.J. (2008) Chromium, chromium isotopes
361 and selected elements, western Mojave Desert, USA. *Appl. Geochem.* **23**, 1325-1352.

362 Johnston, D.T. *et al.* (2005) Active microbial sulfur disproportionation in the
363 Mesoproterozoic. *Science* **310**, 1477-1479.

364 Kah, L.C., Sherman, A.B., Narbonne, G.M., Kaufman, A.J., Knoll, A.H. (1999) $\delta^{13}\text{C}$
365 stratigraphy of the Proterozoic Bylot Supergroup, northern Baffin Island: implications for
366 regional lithostratigraphic correlations. *Can. J. Earth Sci.* **36**, 313-332.

367 Kah, L.C., Lyons, T.W., Chesley, J.T. (2001) Geochemistry of a 1.2 Ga carbonate-
368 evaporite succession, northern Baffin and Bylot Islands: implications for
369 Mesoproterozoic marine evolution. *Precambrian Res.* **111**, 203-234.

370 Kah, L.C., Lyons, T.W., Frank, T.D. (2004) Evidence for low marine sulphate and the
371 protracted oxygenation of the Proterozoic biosphere. *Nature* **431**, 834-838.

372 Levin, L.A. (2003) Oxygen minimum zone benthos: Adaptation and community response
373 to hypoxia. *Oceanogr. Mar. Biol. Annu. Rev.* **41**, 1–45.

374 Liu, X.M. *et al.* (2016) Tracing Earth's O₂ evolution using Zn/Fe ratios in marine
375 carbonates. *Geochemical Perspectives Letters* **2**, 24-34.

376 Lyons, T.W., Reinhard, C.T., Planavsky, N.J. (2014) The rise of oxygen in Earth's early
377 ocean and atmosphere. *Nature* **506**, 307-315.

378 Mills, D.B. *et al.* (2014) Oxygen requirements of the earliest animals. *P. Natl. Acad. Sci.*
379 *USA* **111**, 4168-4172.

380 Mohanta, J., Holmden, C., Blanchon, P. (2016) Chromium isotope fractionation between
381 seawater and carbonate sediment in the Caribbean Sea. *Goldschmidt Abstracts*.

382 Narbonne, G.M. (2005) The Ediacara biota: Neoproterozoic origin of animals and their
383 ecosystems. *Earth Planet. Sci. Lett.* **33**, 421-442.

384 Och, L.M., Shields-Zhou, G.A. (2012) The Neoproterozoic oxygenation event:
385 environmental perturbations and biogeochemical cycling. *Earth-Sci. Rev.* **110**, 26-57.

386 Oze, C., Bird, D.K., Fendorf, S. (2007) Genesis of hexavalent chromium from natural
387 sources in soil and groundwater. *P. Natl. Acad. Sci. USA* **104**, 6544-6549.

388 Palma, M. *et al.* (2005) Macrobenthic animal assemblages of the continental margin off
389 Chile (22° to 42°S). *J. Mar. Biol. Assoc. UK* **85**, 233–245.

390 Parnell, J., Boyce, A.J., Mark, D., Bowden, S., Spinks, S. (2010) Early oxygenation of
391 the terrestrial environment during the Mesoproterozoic. *Nature* **468**, 290-293.

392 Paulukat, C., Frei, R., Voegelin, A.R., Samankassou, E. (2015) Global Cr-isotope
393 distributions in surface seawater and incorporation of Cr isotopes into carbonate shells.
394 *Goldschmidt Abstracts* **2426**.

395 Paulukat, C., Gilleaudeau, G.J., Frei, R. (*in prep.*) The Cr-isotope signature of surface
396 seawater and its relation to the Cr-isotope paleo-redox proxy. *Chem. Geol.*

397 Pavlov, A.A., Kasting, J.F. (2002) Mass-independent fractionation of sulfur isotopes in
398 Archean sediments: strong evidence for an anoxic Archean atmosphere. *Astrobiology* **2**,
399 27-41.

400 Pereira, N.S. *et al.* (2016) Chromium-isotope signatures in scleractinian corals from the
401 Rocas Atoll, Tropical South Atlantic. *Geobiology* **14**, 54-67.

402 Planavsky, N.J. *et al.* (2014) Low mid-Proterozoic atmospheric oxygen levels and the
403 delayed rise of animals. *Science* **346**, 635-638.

404 Rodler, A., Sanchez-Pastor, N., Fernandez-Diaz, L., Frei, R. (2015) Fractionation
405 behavior of chromium isotopes during coprecipitation with calcium carbonate:
406 implications for their use as paleoclimatic proxy. *Geochim. Cosmochim. Ac.* **164**, 221-
407 235.

408 Schoenberg, S., Zink, M., Staubwasser, M., von Blanckenburg, F. (2008) The stable Cr
409 isotope inventory of solid Earth reservoirs determine by double spike MC-ICP-MS.
410 *Chem. Geol.* **249**, 294-306.

411 Scheiderich, K., Amini, M., Holmden, C., Francois, R. (2015) Global variability of
412 chromium isotopes in seawater demonstrated by Pacific, Atlantic, and Arctic Ocean
413 samples. *Earth Planet. Sci. Lett.* **423**, 87-97.

414 Sperling, E.A., Halverson, G.P., Knoll, A.H., Macdonald, F.A., Johnston, D.T. (2013a) A
415 basin redox transect at the dawn of animal life. *Earth Planet. Sci. Lett.* **371-372**, 143-155.

416 Sperling, E.A. *et al.* (2013b) Oxygen, ecology, and the Cambrian radiation of animals. *P.*
417 *Natl. Acad. Sci. USA* **110**, 13446-13451.

418 Spinks, S.C., Parnell, J., Bowden, S.A., Taylor, R.A.D., Maclean, M.E. (2014) Enhanced
419 organic carbon burial in large Proterozoic lakes: implications for atmospheric
420 oxygenation. *Precambrian Res.* **255**, 202-215.

421 Tang, D., Shi, X., Wang, X., Jiang, G. (2016) Extremely low oxygen concentration in
422 mid-Proterozoic shallow seawaters. *Precambrian Res.* **276**, 145-157.

423 Taylor, S.R., McLennan, S.M. (1985) The continental crust: its composition and
424 evolution. *Blackwell Scientific Publications*, Palo Alto, CA.

425 Wang, X. *et al.* (2016) Chromium isotope fractionation during subduction-related
426 metamorphism, black shale weathering, and hydrothermal alteration. *Chem. Geol.* **423**,
427 19-33.

428 Wedepohl, K.H. (1991) The composition of the upper Earth's crust and the natural cycles
429 of selected metals. Metals in natural raw materials. Natural resources. In E. Merian *et al.*
430 (eds.), *Metals and their compounds in the environment: occurrence, analysis, and*
431 *biological relevance*. VCH. Weinheim, New York, Basel, Cambridge, 3-17.

432 Zhang, S. *et al.* (2016) Sufficient oxygen for animal respiration 1,400 million years ago.
433 *P. Natl. Acad. Sci. USA* **113**, 1731-1736.

Figure 1

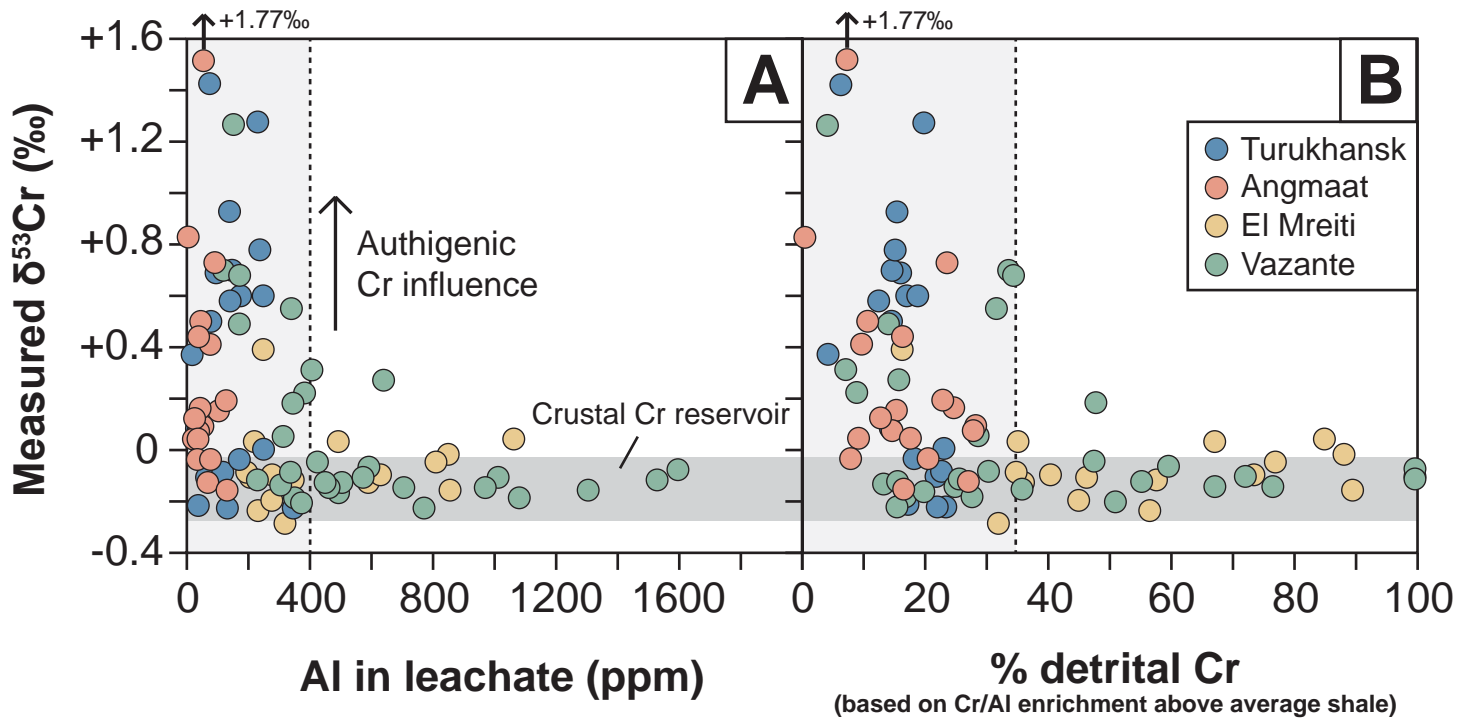


Figure 2

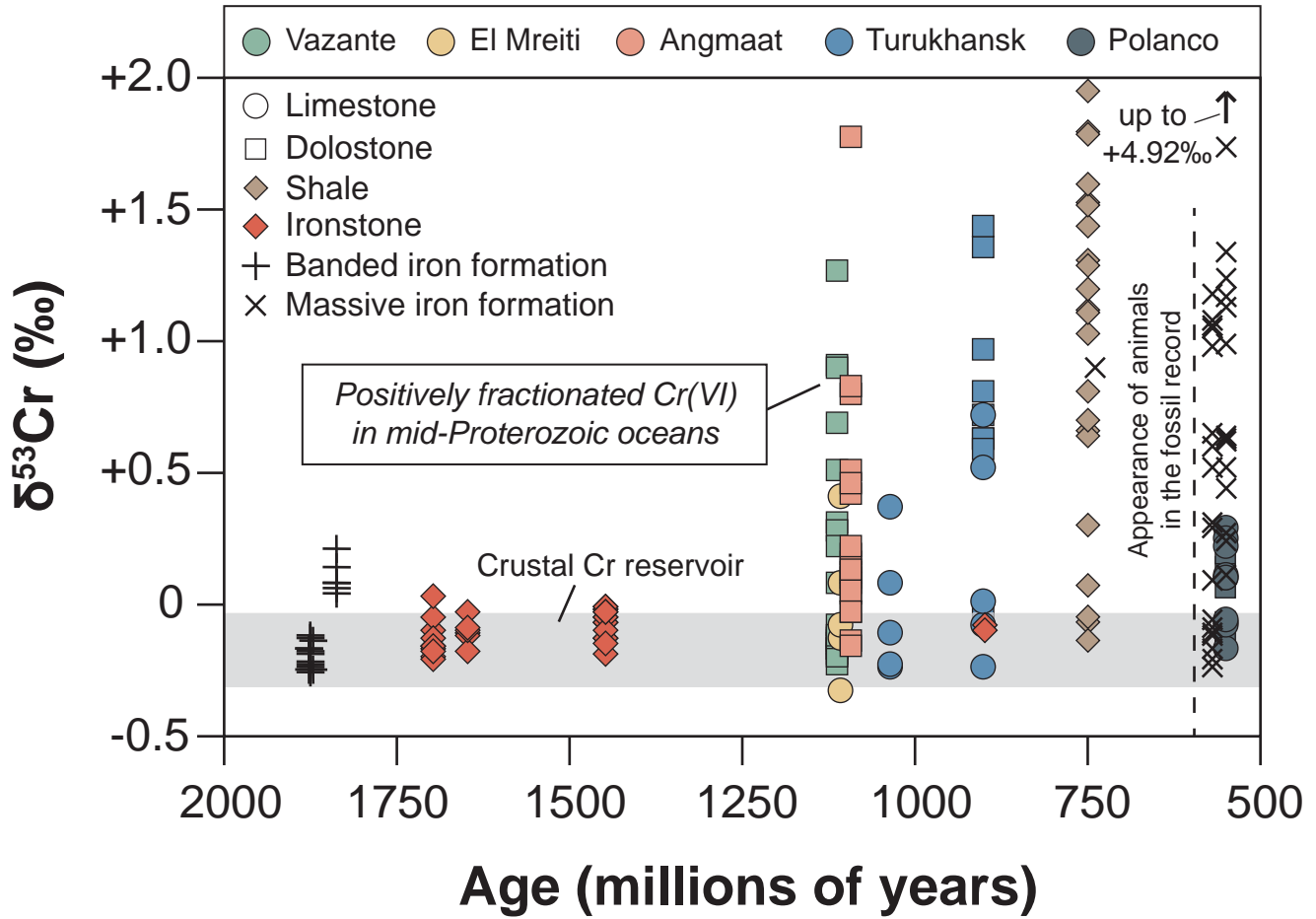


Figure SI-1

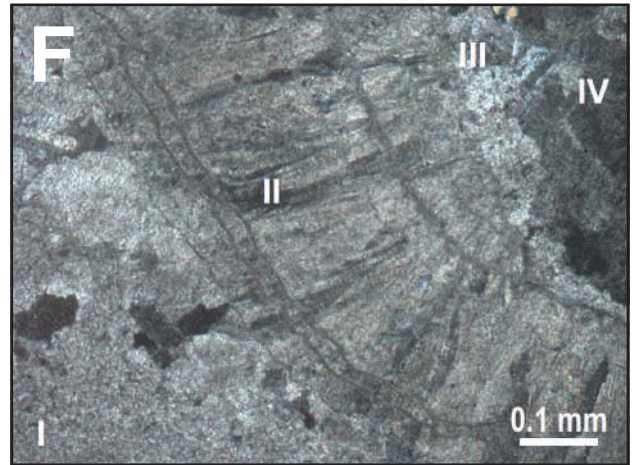
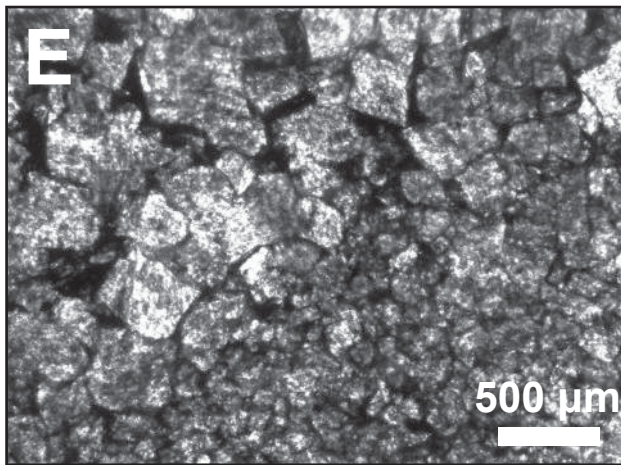
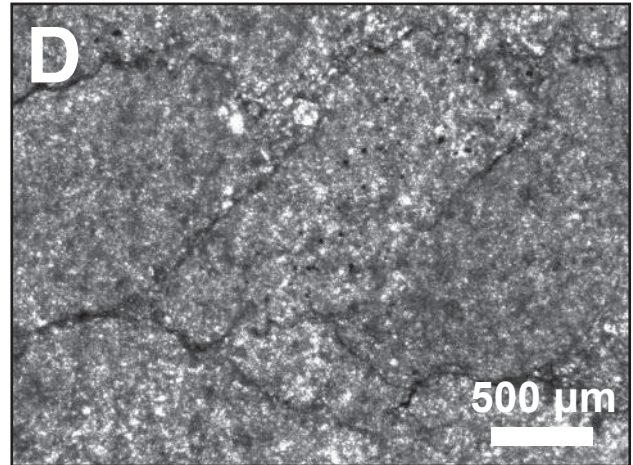
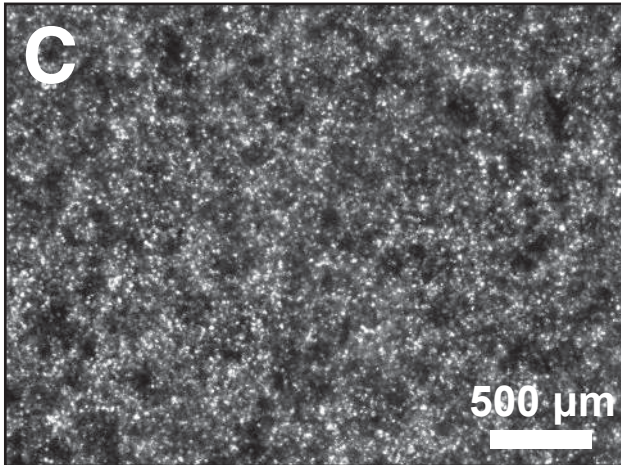
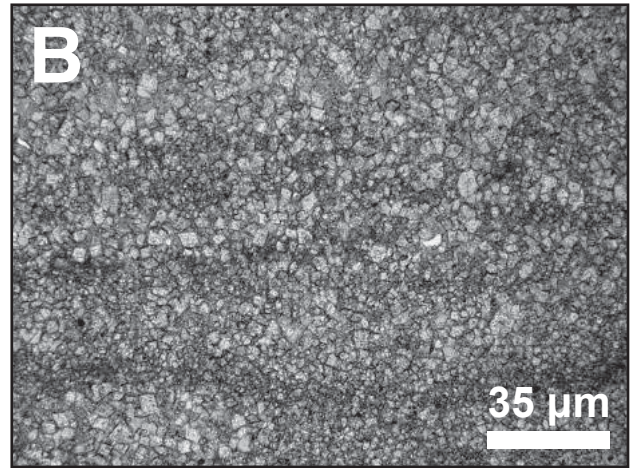
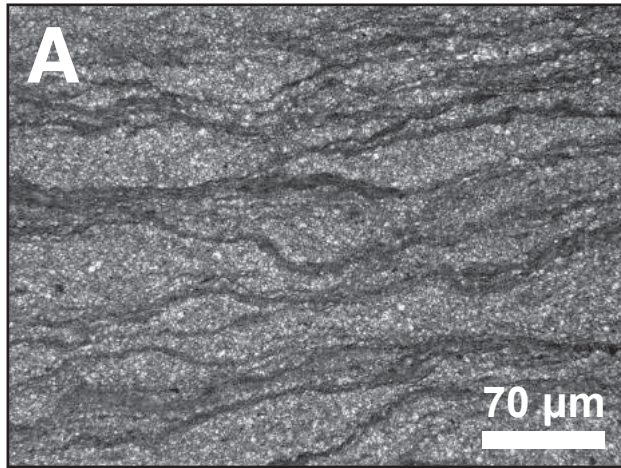


Figure SI-2

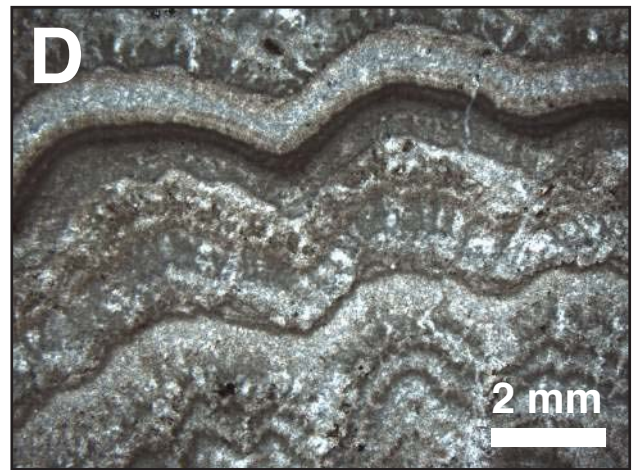
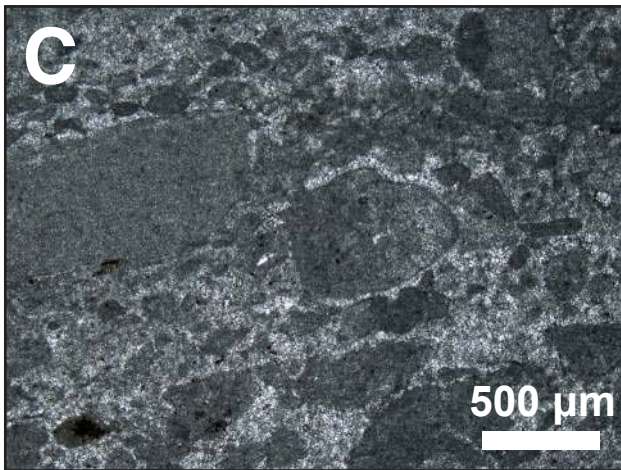
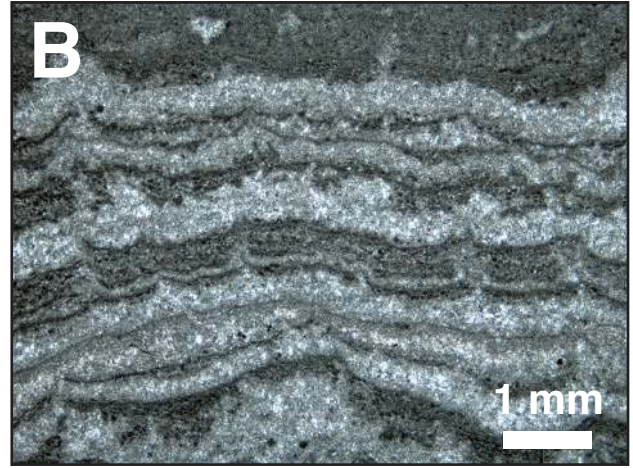
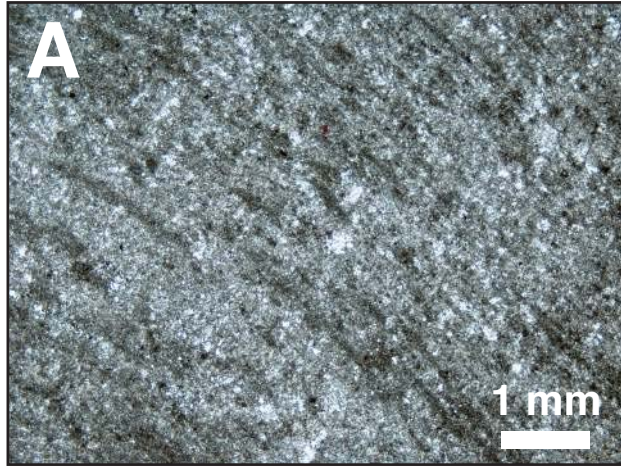


Figure SI-3

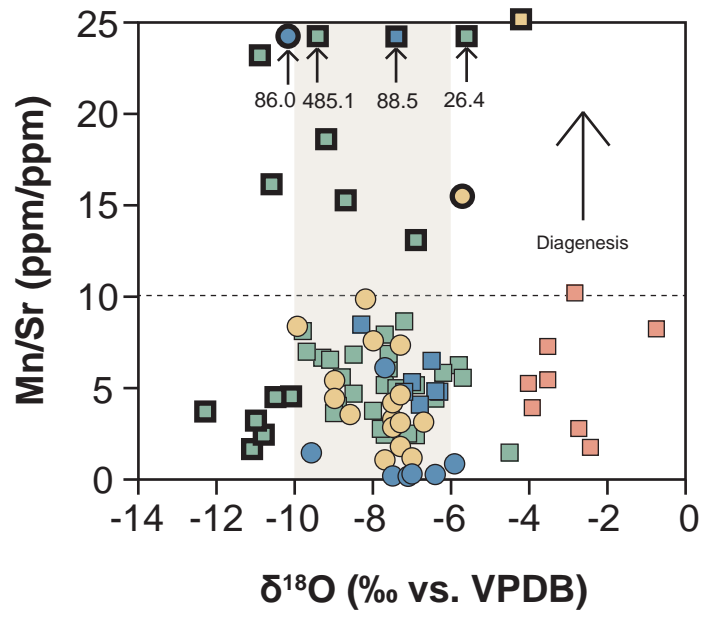
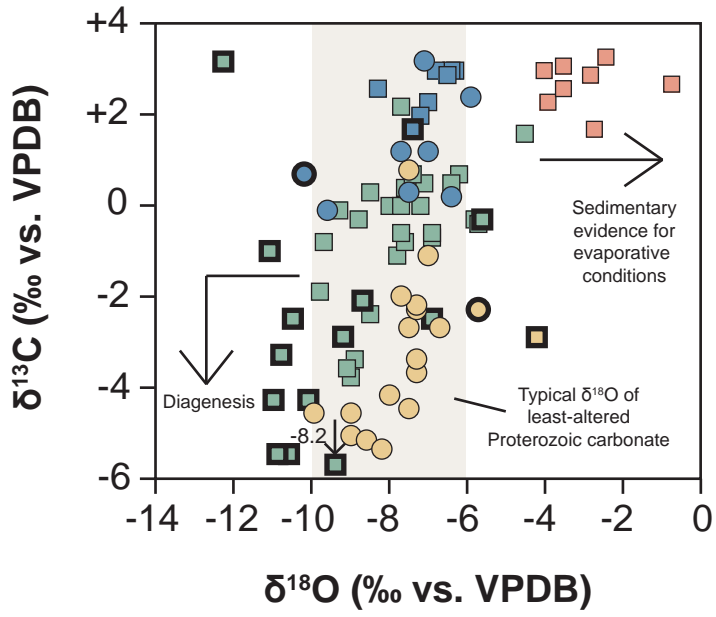


Figure SI-4

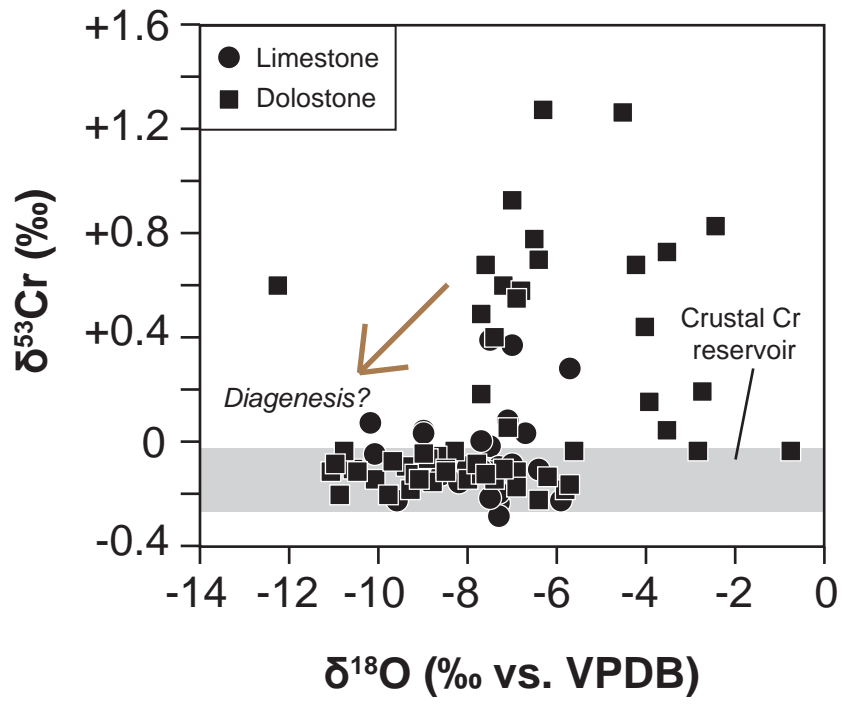


Figure SI-5

